

Published in final edited form as:

Nat Neurosci. 2015 May ; 18(5): 628–630. doi:10.1038/nn.3991.

Synaptic vesicle release regulates the number of myelin sheaths made by individual oligodendrocytes in vivo

Sigrid Mensch¹, Marion Baraban¹, Rafael Almeida¹, Tim Czopka^{1,3}, Jessica Ausborn², Abdel El Manira², and David A Lyons¹

¹Centre for Neuroregeneration, Centre for Multiple Sclerosis Research, Euan MacDonald Centre for Motor Neurone Disease Research, University of Edinburgh, 49 Little France Crescent, Edinburgh EH16 4SB, UK.

²Department of Neuroscience, Karolinska Institute, 171 77 Stockholm, Sweden.

Abstract

The myelination of axons by oligodendrocytes profoundly affects central nervous system function, but how this is regulated by neuronal activity in vivo is not known. Here we find that blocking synaptic vesicle release impairs CNS myelination by reducing the number of myelin sheaths made by individual oligodendrocytes during their short period of formation. We also find that stimulating neuronal activity increases myelin sheath formation by individual oligodendrocytes. These data show that neuronal activity regulates the myelinating capacity of single oligodendrocytes.

CNS myelination continues into adult life¹⁻³ and previous studies have suggested that neuronal activity may regulate myelination (e.g.⁴⁻⁶) and in turn nervous system plasticity^{7,8}. Studies in humans have shown that the execution of specific tasks can promote the growth of white matter in relevant brain areas⁹. Furthermore, rodent models have revealed that the social environment influences the amount of myelin made by individual oligodendrocytes¹⁰, and that learning specific tasks stimulates and requires the generation of new myelinating oligodendrocytes¹¹. However, how neuronal activity might regulate the myelinating capacity of individual oligodendrocytes in vivo has remained unclear. We have previously shown that the presence of supernumerary axons in the zebrafish spinal cord can stimulate individual oligodendrocytes to generate more myelin sheaths than they would otherwise, indicating that axons can regulate the myelinating potential of individual oligodendrocytes in vivo¹². Here we test the possibility that neuronal activity might regulate myelin sheath generation by individual oligodendrocytes during their previously characterised short period of sheath formation in vivo^{13,14}.

Using zebrafish as a model organism, we used tetanus toxin (TeNT) to abrogate synaptic vesicle release in vivo¹⁵. Electrophysiology confirmed a reduction in synaptic activity

Users may view, print, copy, and download text and data-mine the content in such documents, for the purposes of academic research, subject always to the full Conditions of use:http://www.nature.com/authors/editorial_policies/license.html#terms

³Current address: Institute of Neuronal Cell Biology, Technical University Munich, Biedersteiner Str. 29, 80802 Munich, Germany

A supplementary methods checklist is available as part of the supplementary information.

without disruption to general morphological development (See Online Methods, Fig. 1a and Supplementary Figures 1 + 2). To visualise myelination in live animals we used Tg(mbp:mCherry-CAAX) and Tg(mbp:EGFP-CAAX), which revealed that although the onset of myelination was not delayed there was a reduction in the amount of myelin in TeNT expressing animals (Fig. 1b and Supplementary Fig. 2). By Transmission Electron Microscopy (TEM) we observed a 39 % decrease in the number of myelinated axons in TeNT expressing animals (67 \pm 9 control vs 41 \pm 9 TeNT) and a concomitant increase in the number of unmyelinated axons $> 0.3 \mu\text{m}$ in calibre (the diameter of the smallest myelinated axons) (37 \pm 6 control vs 70 \pm 12 TeNT) (Fig. 1c – e and Supplementary Fig. 3). Importantly, we found that the number (104.4 \pm 12.2 control vs 110.8 \pm 13.3 TeNT), size, and distribution of axons $> 0.3 \mu\text{m}$ was unchanged by TeNT treatment at 4 dpf (Fig. 1e and Supplementary Fig. 3). These results show that disruption of synaptic vesicle release does not affect the early development of axons or the growth in calibre of CNS axons in vivo, but does affect their myelination.

To elucidate this observed reduction in myelinated axon number, we first quantified myelinating oligodendrocytes, because numerous studies have implicated neuronal activity in the regulation of oligodendrocyte number^{6,16}. Using Tg(mbp:EGFP) to count myelinating oligodendrocytes, we found a small (10 %) reduction in their number by 4 dpf in TeNT expressing animals (49 \pm 9 control vs 44 \pm 9 TeNT) (Supplementary Fig. 4). In order to determine whether this reduction reflected changes in Oligodendrocyte Precursor Cell (OPC) proliferation, survival or differentiation we carried out time-course and time-lapse analyses from OPC specification onwards (see Online Methods). Interestingly, we found a 10 % decrease in cell number from the earliest appearance of OPCs suggesting that the reduction in cell number results from disruption to specification in the pMN domain (Supplementary Fig. 5). Indeed, a role for neurotransmitters in modulation of pMN domain behaviour in zebrafish has recently been demonstrated with respect to the generation of motor neurons¹⁷. Time-lapse analyses revealed no differences in later OPC proliferation or survival in TeNT expressing animals (Supplementary Fig. 5 and Supp. Movies 1 + 2 and data not shown). It is important to note that rates of OPC proliferation and cell death are low in zebrafish at the stages examined (Supplementary Fig. 5, Supp. Movies 1 + 2). Therefore the modest phenotype in cell number observed in our study may reflect difference in scale, rather than principle, between species.

Given that the 10 % reduction in oligodendrocyte number does not account for the 40 % reduction in myelinated axons observed at 4 dpf, we reasoned that individual oligodendrocytes must either have fewer myelin sheaths, or significantly shorter sheaths in TeNT expressing animals. Therefore, we next assessed individual oligodendrocyte morphology using mbp:mCherry-CAAX. We found that the average number of myelin sheaths per oligodendrocyte at 4 dpf was reduced by 30 % in TeNT expressing animals (11.9 \pm 3.1 sheaths per cell control vs 8.2 \pm 2.9 TeNT) (Fig. 2a,b). Of the myelin sheaths that did form in the global absence of synaptic vesicle release, we did not observe any statistically significant decrease in their length at 4 dpf (Supplementary Fig. 6). To determine whether the reduction in myelin sheath number per cell was due to a defect in their initial formation or an increase in retraction we performed time-lapse imaging of individual oligodendrocytes using Tg(nkx2.2a:mEGFP), as previously¹³, whereby we

define myelin sheaths as elongate structures with characteristic ensheathing profiles $> 5 \mu\text{m}$ in length that are stable for > 10 minutes. By the end of the characteristic short period of myelin sheath generation, which was unchanged in TeNT expressing animals (Figure 2 c – e), we saw that individual oligodendrocytes had generated 30 % fewer myelin sheaths (9.5 ± 2.0 , control vs 6.7 ± 2.3 , TeNT) in TeNT expressing animals; no difference was observed in the number of myelin sheath retractions (3.1 ± 1.2 , control vs 3.5 ± 1.2 , TeNT, Fig. 2 c – f Supp. Movie 3 + 4).

Together the 10 % reduction in oligodendrocyte number and the 30 % decrease in myelin sheath number per cell account for the 40 % reduction in myelinated axon number seen by TEM.

To exclude the possibility that the effect on myelin sheath generation is due to the function of TeNT in oligodendrocytes^{18,19}, we created genetic chimeras (See Online Methods). When TeNT expressing oligodendrocytes were placed into a control axonal environment we found that they generated a normal number of myelin sheaths (average of 12 ± 2.7 per cell) (Supplementary Fig. 7). In contrast, when we analysed control oligodendrocytes in TeNT expressing animals with reduced synaptic vesicle release, we observed reduced myelin sheath number (average of 8.6 ± 3.3 per cell), (Supplementary Fig. 7). These analyses show that TeNT does not function in oligodendrocytes to regulate myelin sheath formation. To demonstrate that disruption of synaptic vesicle release specifically in neurons regulates myelin sheath formation, we drove expression of TeNT in individual reticulospinal neurons and found that this led to the formation of 40 % fewer myelin sheaths along their axons (Supplementary Fig. 8). Together these data indicate that synaptic vesicle release from axons regulates myelin sheath formation.

Given that a decrease in synaptic vesicle release caused a profound reduction in myelin sheath number per oligodendrocyte, we next asked whether an increase in neuronal activity might promote myelin sheath production by oligodendrocytes. In order to induce neuronal gain of function we used the GABA-A receptor antagonist pentylenetetrazole (PTZ), which has previously been shown to disinhibit the firing of reticulospinal neurons, and which we show augments the characteristic escape responses mediated by myelinated reticulospinal axons in the ventral spinal cord (Supplementary Fig. 9, Supp. Movies 5 + 6, and Online Methods). We found that PTZ treatment caused a subtle but significant increase in the number of oligodendrocytes in the ventral spinal cord, where reticulospinal axons are located (45 ± 6 oligodendrocytes control vs 48 ± 8 PTZ) (Supplementary Fig. 9). Importantly, we observed a roughly 40 % increase in the number of myelin sheaths made by individual oligodendrocytes in the ventral spinal cord following PTZ treatment (Figure 3 and Supplementary Fig. 9). We confirmed that this increase was due to synaptic vesicle release by showing that the PTZ-induced increase in sheath number was entirely eliminated by expression of TeNT in PTZ treated animals (Figure 3) (10.9 ± 3.5 sheaths per cell control, 14.8 ± 2.4 PTZ and 10.1 ± 3.5 PTZ + TeNT). These experiments indicate that an increase in neuronal activity promotes myelin sheath production by individual oligodendrocytes in a synaptic vesicle release dependent manner.

Future studies will reveal the underlying mechanisms by which neuronal activity regulates myelin sheath formation by oligodendrocytes. One possibility is that synaptic vesicle release functions through direct synaptic contacts between axons and the processes of oligodendrocytes and that such synapses regulate the initial formation or stabilisation of axon-OL contacts, or their subsequent transformation into myelin sheaths²⁰. Alternatively synaptic vesicle release could either locally influence individual oligodendrocyte process behaviour in an extra-synaptic manner or individual oligodendrocytes could recognise the cumulative level of synaptic vesicle release in their environment and integrate this information to regulate their overall gain of myelination.

In summary, our data show that synaptic vesicle release affects the myelinating capacity of individual oligodendrocytes during their initial period of sheath formation, providing novel insight into activity dependent myelination.

Online Methods

Fish husbandry

All animals used in this study were maintained under standard conditions (Westerfield, 1995) and all experiments performed according to the British Home Office regulations. The following already published transgenic zebrafish lines were used: Tg(*nkx2.2a:mEGFP*)^{21,22}, Tg(*sox10:mRFP*)²¹, Tg(*olig2:EGFP*)²³, Tg(*mbp:EGFP-CAAX*) and Tg(*mbp:EGFP*)¹², and Tg(*cntn1b(5kb):mCherry*)¹³. Tg(*mbp:mCherry-CAAX*) and Tg(*HuC:Gal4*) was generated for the purpose of this study by screening founders derived following co-injection of 1nl of 10 ng/μl plasmid DNA encoding *mbp:mCherry-CAAX* and *HuC:Gal4* respectively with 25 ng/μl *tol2* transposase mRNA.

Calibration of tetanus toxin concentration using electrophysiology

To inhibit synaptic vesicle release, fertilized eggs were injected with 1 nl of either 10, 50 or 100 ng/μl of mRNA encoding a fusion protein between EGFP and the Tetanus Toxin Light Chain (*tent-lc:EGFP*) at the 1 – 4 cell stage²⁴. Controls were injected at the same developmental stage with 1nl of nuclease free water. All embryos were manually dechorionated at 1 day post fertilisation.

At 4 days post fertilization (dpf) fish were anesthetized in 0.03 % Tricaine (MS-222, Sigma) in extracellular solution and then pinned down on the side using tungsten pins placed through the notochord in a Sylgard-lined recording chamber. The fish were paralyzed with 6.25 μM α-bungarotoxin (Sigma-Aldrich) for 10 minutes and muscles were removed over one segment to record from spinal cord neurons. Patch-clamp electrodes were pulled from borosilicate glass (1.5 mm outer diameter, 0.87 mm inner diameter, Hilgenberg). The intracellular solution (120 mM potassium gluconate, 5 mM KCl, 10 mM HEPES, 4 mM ATP-Mg²⁺, 0.3 mM GTP-Na⁺, 10 mM Na⁺-phosphocreatine, pH 7.4 with KOH, 275 mOsm), yielding resistances of 8 – 12 MΩ. Synaptic activity was induced in spinal neurons by electrical stimulation using a glass electrode placed at the level of the otic vesicle. The synaptic activity of spinal cord neurons was examined in current-clamp and in voltage-clamp. Inward excitatory currents were recorded in neurons held at –65 mV, which

corresponds to the reversal potential of chloride-mediated inhibition. Outward inhibitory currents were recorded in neurons held at 0 mV, which corresponds to the reversal potential of excitation.

Only animals injected with 100 ng/μl *tent-lc:EGFP* mRNA exhibited consistent blockade of synaptic transmission, despite those injected with the lower dose being paralysed (data not shown). Therefore 1 nl of 100 ng/μl was used throughout all experiments. Although encoding a EGFP fusion protein, for simplicity we refer to TeNT treatment throughout.

Single oligodendrocyte labelling

To generate mosaically labelled oligodendrocytes fertilized eggs were injected with 10 ng/μl plasmid DNA encoding mbp:mCherry-CAAX and 25 ng/μl transposase mRNA at the 1 – 8 cell stage. To generate a mbp:mCherry-CAAX transgenic construct, we recombined p5E_mbp¹² with pME_mCherry-CAAX, p3E_pA, and pDestTol2pA2 (all from Tol2Kit, ²⁵).

Generation of genetic chimeras

To generate genetic chimeras we carried out cell transplantation at blastula stages. We transplanted cells from control to control, from TeNT expressing animals to control, and from control to TeNT expressing animals. Donor embryos were labelled with either 0.2 % (w/v) Oregon Green Dextran or 0.2 % Cascade Blue Dextran. For control to control and TeNT to control chimeras donor embryos were Tg(mbp:EGFP-CAAX) in order to be able to easily quantify myelin sheath number per cell in the host. For control to TeNT chimeras the donor embryos were Tg(sox10:mRFP) in order to be able to easily quantify myelin sheath number in the host TeNT animal, which expresses a low level of EGFP because of the TeNT-LC:EGFP fusion protein. Quantification of myelin sheath number was performed whilst blinded to experimental group.

Expression and analysis of TeNT in individual Reticulospinal Neurons

In order to express TeNT in individual neurons we injected UAS:TeNT-TdTomato (kind gift of Martin Meyer) into Tg(HuC:Gal4), Tg(mbp:EGFP-CAAX) double transgenic lines. As controls we injected UAS:TdTomato into Tg(HuC:Gal4), Tg(mbp:EGFP-CAAX) double transgenic lines. To generate Tg(HuC:Gal4) we subcloned the zebrafish HuC promoter (kind gift of Martin Meyer) into pDONR_P4-P1R to generate p5E_huC using the following primers: attB4_huc_F:

GGGGACAACCTTTGTATAGAAAAGTTGGAATTCACCTAATTTG AATTTAAATGC,

attB1R_huc_R: *GGGGACTGCTTTTTGTACAAACTTGTC*

TTGACGTACAAAGATGATATG. PTol2_huc:Gal4-VP16 created by recombining standard components of the Tol2kit²⁵. We screened for TdTomato and TeNT-TdTomato expression in neurons with large caliber RS axons, based on their known morphology²⁶, prior to blinded analyses of their myelination from somite levels 8 – 16. Quantification of myelin sheath number along single axons was performed whilst blinded to experimental group.

Pentylentetrazole treatment

Pentylentetrazole (PTZ) is a well characterised GABA-A receptor antagonist²⁷. Previous studies using zebrafish have shown that PTZ can induce increases in neuronal activity and exacerbated response to touch stimuli at concentrations up to 2.5 mM and can induce seizures at higher concentrations²⁸. Previous studies have also indicated that reticulospinal neurons receive significant inhibitory GABA-ergic input^{29,30}, making PTZ a strong candidate to induce a gain of function in reticulospinal axons that could in turn regulate oligodendrocyte behaviour. We next reasoned that it would be important to induce a gain of function throughout a period that would encompass all stages of oligodendrocyte development from specification from the pMN domain, migration to axonal tracts, proliferation, survival, differentiation and ultimately myelination (from 2 dpf through 4 dpf). We found that zebrafish tolerated long-term treatment with PTZ up to 2.5 mM without significant deleterious effects to morphological development or maturation, or any evidence of seizing. We selected morphologically normal and healthy animals for cellular analyses. To confirm that animals treated with 2 mM PTZ exhibited an exaggerated response to touch as previously indicated, we quantified the swim distance swam in animals responding to touch using Noldus Ethovision XT and ImageJ. Quantification of oligodendrocyte number in control and PTZ treated Tg(mbp:EGFP) animals as well as the quantification of myelin sheath number in single mbp:mCherry-caax labelled oligodendrocytes in control, PTZ, PTZ and TeNT treated animals was performed while blinded to the treatment group.

Transmission Electron Microscopy

Tissue was prepared for transmission electron microscopy (TEM) as previously described³¹ and sectioned using a Reichert Jung Ultracut Microtome. TEM images were taken with a Phillips CM120 Biotwin TEM. Image analysis was performed using ImageJ and Adobe Photoshop CS3.

Live imaging and data analysis

Embryos were embedded in 1.3 – 1.5 % low melting point agarose (Invitrogen) in embryo medium with MS-222 (tricaine methane-sulfonate, Sigma-Aldrich). All fluorescent live images and time-lapse movies represent a lateral view of the spinal cord, anterior to the left and dorsal on top. Confocal images and time-lapses were acquired using Zeiss LSM 710 and 780 confocal microscopes. During time-lapses the agarose embedded fish were staged on a Tempcontrol 37 temperature controlled microscope stage at 28 °C to keep the fish under optimal conditions. The time-lapse movies were acquired at time intervals of 10 min between each frame.

Images of individual cells in the figure panels are labelled by mbp:mCherry-CAAX, while images of stable transgenic lines are labelled by the “Tg” designation indicating a transgenic line, e.g. Tg(mbp:mCherry-CAAX).

All timelapse analysis and colour coding in the figure panels was carried out using ImageJ and Adobe Photoshop CS3.

Statistical analyses

All data are expressed as a mean \pm standard deviation or as relative proportions of 100 % as indicated in the appropriate legends. For statistical analyses, either a Student's two-tailed t-test, a one-way or two-way ANOVA was used, as indicated in the figure legends. All graphs and statistical tests were carried out using either GraphPad Prism 5 or Microsoft Excel 2010. Statistical significance abbreviations are used as follows: * = $p < 0.05$, ** = $p < 0.01$, *** = $p < 0.001$. Samples in our data sets were not randomized and the analysis was not blinded unless otherwise stated above. Data distribution was assumed to be normal but this was not formally tested.

Sample size was determined by power analysis. 100 % power was achieved in the quantification of myelin sheaths per oligodendrocytes in figure 2b. 100 % power was achieved in the quantification of myelin sheaths along the axons in Supp. figure 8b. 100 % power was achieved in the quantification of myelin sheaths per oligodendrocyte in supp. figure 9e. 99 % power was achieved in the quantification of oligodendrocytes in the ventral spinal cord shown in supp. figure 9g. 100 % power was achieved in figure 1d. 97 % power was achieved in the number of sheaths formed during time-lapse analysis shown in figure 2f. 80 % power was achieved in the number of oligodendrocytes shown in supp. figure 4b.

Supplementary Material

Refer to Web version on PubMed Central for supplementary material.

Acknowledgments

We thank Dr. Martin Meyer for reagents and Dr. Carl Tucker and staff for fish care. This work was supported by a Wellcome Trust Senior Fellowship, a BBSRC David Phillips Fellowship and a Lister Research Prize to D.A.L.

References

1. Wang S, Young KM. *Neuroscience*. 2014; 276:148–160. [PubMed: 24161723]
2. Yeung MSY, et al. *Cell*. 2014; 159:766–774. [PubMed: 25417154]
3. Young KM, et al. *Neuron*. 2013; 77:873–885. [PubMed: 23473318]
4. Demerens C, et al. *Proceedings of the National Academy of Sciences of the United States of America*. 1996; 93:9887–9892. [PubMed: 8790426]
5. Wake H, Lee PR, Fields RD. *Science*. 2011; 333:1647–1651. [PubMed: 21817014]
6. Gibson EM, et al. *Science*. 2014; 344:1252304. [PubMed: 24727982]
7. de Hoz L, Simons M. *Bioessays*. 2015; 37:60–69. [PubMed: 25363888]
8. Fields RD. *Science*. 2010; 330:768–769. [PubMed: 21051624]
9. Zatorre RJ, Fields RD, Johansen-Berg H. *Nat Neurosci*. 2012; 15:528–536. [PubMed: 22426254]
10. Makinodan M, Rosen KM, Ito S, Corfas G. *Science*. 2012; 337:1357–1360. [PubMed: 22984073]
11. McKenzie IA, et al. *Science*. 2014; 346:318–322. [PubMed: 25324381]
12. Almeida RG, Czopka T, Ffrench-Constant C, Lyons DA. *Development*. 2011; 138:4443–4450. [PubMed: 21880787]
13. Czopka T, Ffrench-Constant C, Lyons DA. *Developmental Cell*. 2013; 25:599–609. [PubMed: 23806617]
14. Watkins TA, Emery B, Mulinyawe S, Barres BA. *Neuron*. 2008; 60:555–569. [PubMed: 19038214]

15. Asakawa K, et al. Proceedings of the National Academy of Sciences of the United States of America. 2008; 105:1255–1260. [PubMed: 18202183]
16. Barres BA, Raff MC. Nature. 1993; 361:258–260. [PubMed: 8093806]
17. Reimer MM, et al. Developmental Cell. 2013; 25:478–491. [PubMed: 23707737]
18. Sloane JA, Vartanian TK. Journal of Neuroscience. 2007; 27:11366–11375. [PubMed: 17942731]
19. Feldmann A, et al. Journal of Neuroscience. 2011; 31:5659–5672. [PubMed: 21490207]
20. Almeida RG, Lyons DA. Neuroscience. 2014; 276:98–108. [PubMed: 24035825]

Methods References

21. Kirby BB, et al. Nat Neurosci. 2006; 9:1506–1511. [PubMed: 17099706]
22. Ng AN, et al. Dev. Biol. 2005; 286:114–135. [PubMed: 16125164]
23. Shin J, Park HC, Topczewska JM, Mawdsley DJ, Appel B. Methods Cell Sci. 2003; 25:7–14. [PubMed: 14739582]
24. Ben Fredj N, et al. Journal of Neuroscience. 2010; 30:10939–10951. [PubMed: 20702722]
25. Kwan KM, et al. Dev. Dyn. 2007; 236:3088–3099. [PubMed: 17937395]
26. Gahtan E, O'Malley DM. J. Comp. Neurol. 2003; 459:186–200. [PubMed: 12640669]
27. Huang RQ, et al. J. Pharmacol. Exp. Ther. 2001; 298:986–995. [PubMed: 11504794]
28. Baraban SC, Taylor MR, Castro PA, Baier H. Neuroscience. 2005; 131:759–768. [PubMed: 15730879]
29. Korn H, Faber DS. Neuron. 2005; 47:13–28. [PubMed: 15996545]
30. Nakayama H, Oda Y. Journal of Neuroscience. 2004; 24:3199–3209. [PubMed: 15056699]
31. Czopka T, Lyons DA. Methods in cell biology. 2011; 105:25–62. [PubMed: 21951525]

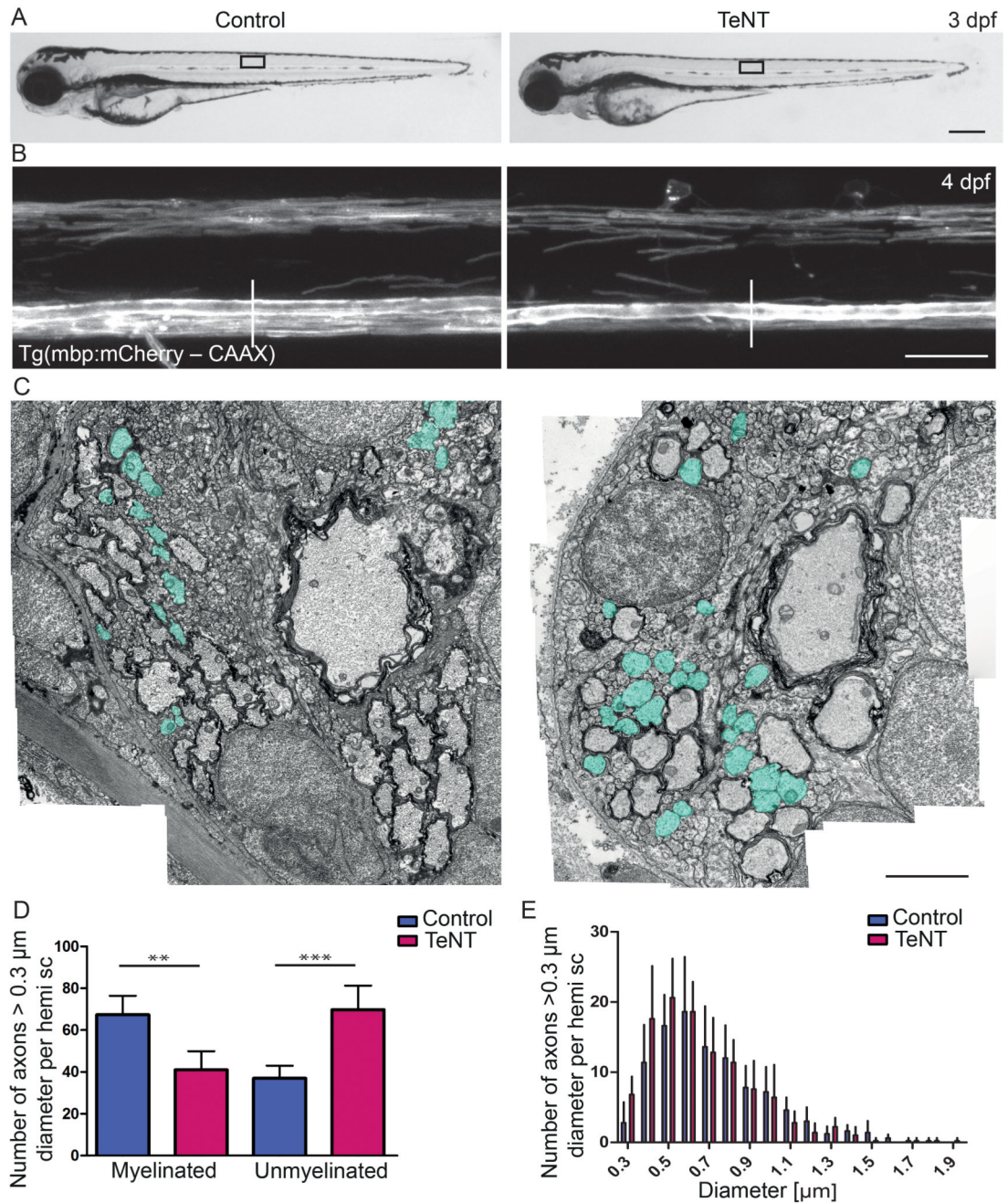


Figure 1. Synaptic vesicle release regulates myelinated axon number

(a) Lateral view of control (left) and TeNT expressing (right) zebrafish at 3 dpf. Boxes indicate areas in b. (Scale bar 250 μm)

(b) Lateral view of Tg(mbp:mCherry-CAAX) spinal cords in controls (left) and TeNT expressing animals (right) (Scale bar 25 μm). White lines indicate the areas of ventral spinal cord illustrated in c.

(c) Transmission electron micrographs of control (left) and TeNT expressing (right) animals at 4 dpf (Scale bar 2 μm). Unmyelinated axons > 0.3 μm diameter indicated in turquoise.

(d) Number of myelinated and unmyelinated axons $> 0.3 \mu\text{m}$ diameter in control and TeNT expressing hemi-spinal cords (Student's two-tailed t-tests, myelinated axon number $p = 0.0017$, unmyelinated axon number, $p = 0.0005$, total axon $> 0.3 \mu\text{m}$ number $p = 0.4$, control $n = 5$, TeNT $n = 5$).

(e) Axon diameter distribution of axons between $0.3 \mu\text{m}$ and $1.9 \mu\text{m}$ (control $n = 5$, TeNT $n = 5$).

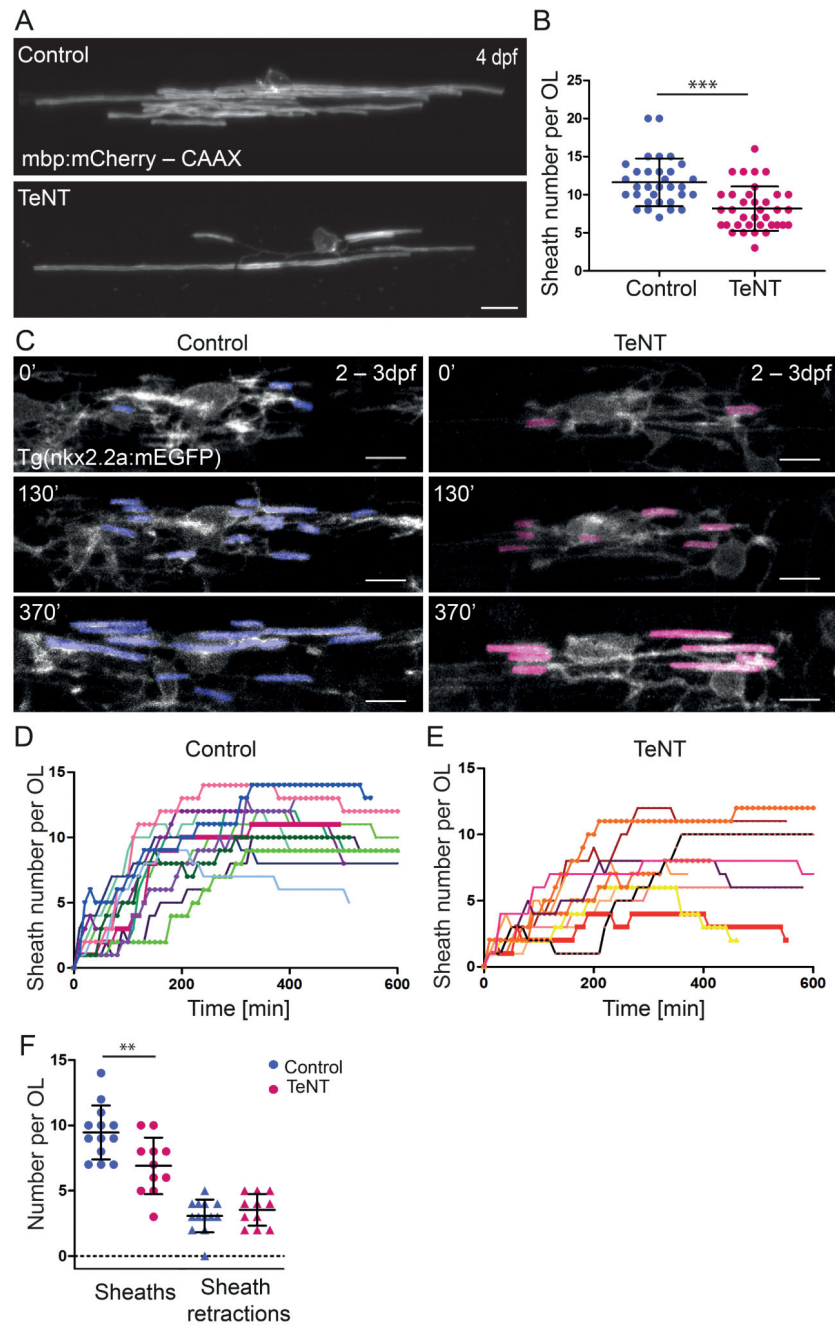


Figure 2. Synaptic vesicle release regulates myelin sheath formation by individual oligodendrocytes

(a) Individual oligodendrocytes labelled by mbp:mCherry-CAAX in control (top), and TeNT (bottom) animals at 4 dpf. Scale bar 10 μ m.

(b) Myelin sheath number per cell (oligodendrocytes in dorsal plus ventral spinal cord) (Student's two-tailed t-test, $p = 1.23872E-05$, $n = 45$ cells in 24 animals; TeNT, $n = 47$ cells in 26 animals).

(c) Time-lapse images of oligodendrocytes in a control (left) and TeNT expressing animal (right). Scale bar 10 μ m. The colours in d correspond to relevant traces in D and E.

(d + e) Total number of myelin sheaths for 13 different control (d) and 11 TeNT (e) oligodendrocytes over time. Time point zero is the time at which each individual oligodendrocyte initiates formation of its first myelin sheath.

(f) Number of myelin sheaths per oligodendrocyte 6 hours after initiation of first myelin sheath, and number of sheath retractions within that 6 hour period of sheath generation (Student's two-tailed t-test, $p = 0.007$ for sheath number and $p = 0.55$ for sheath retraction, $n = 13$ cells in 13 control and $n = 11$ cells in 11 in TeNT expressing animals).

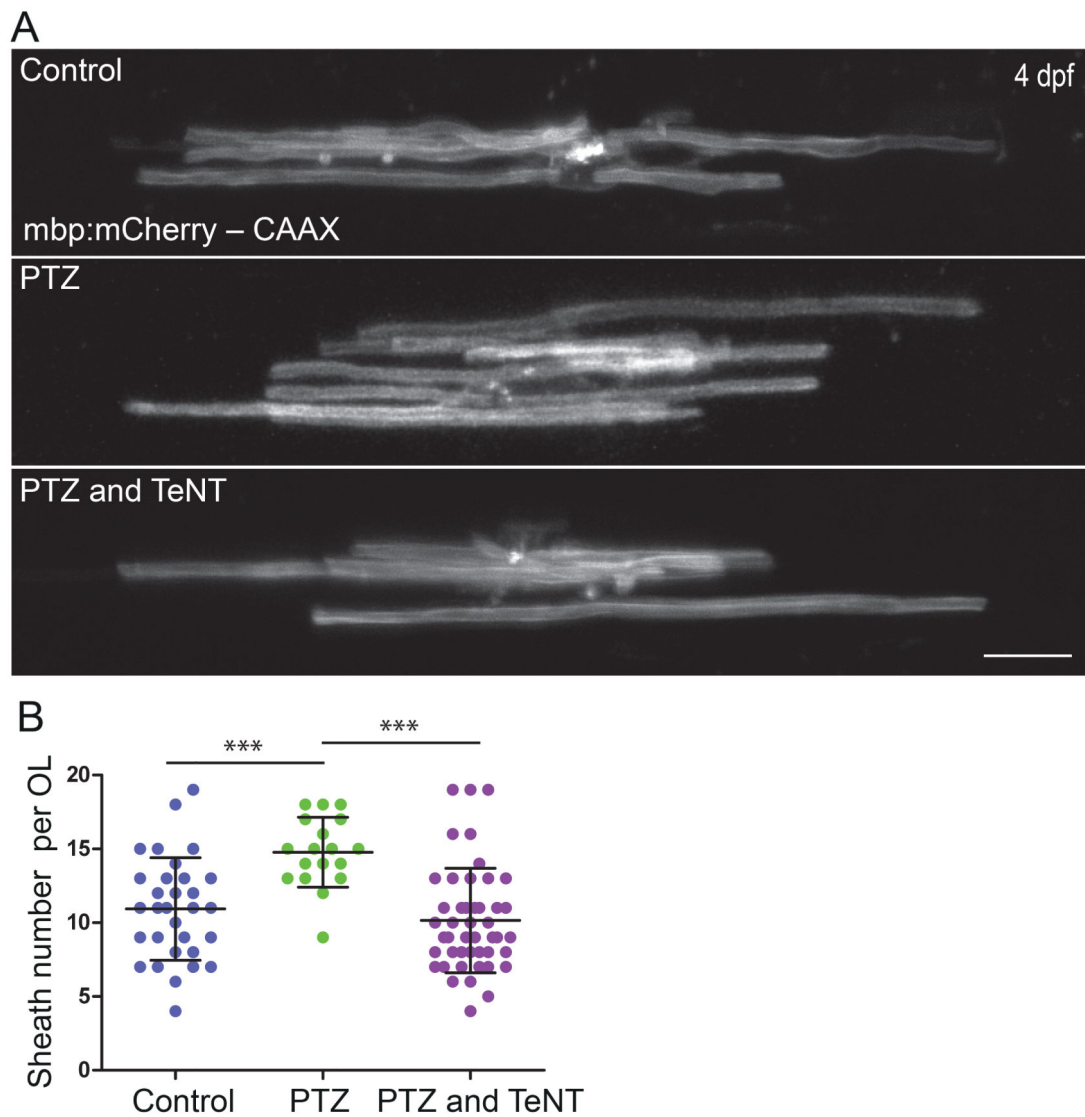


Figure 3. Pentylentetrazole increases myelin sheath number per oligodendrocyte in a synaptic vesicle dependent manner

(a) Individual oligodendrocytes in the ventral spinal cord labelled by mbp:mCherry-CAAX in control (top), PTZ (middle) and PTZ + TeNT (bottom) treated animals at 4 dpf. Scale bar 10 μ m.

(b) Myelin sheath number per cell (oligodendrocytes in ventral spinal cord) (One way ANOVA, $p = 1.32E-05$: Student's two-tailed t-tests, Control vs PTZ, $p = 0.0001$, PTZ vs PTZ+TeNT, $p = 3.40762E-06$, Control $n = 31$, cells in 25 animals; PTZ, $n = 18$ cells in 14 animals, PTZ + TeNT $n = 46$ cells in 29 animals).